Secretome Dynamics in a Gram-Positive Bacterial Model

Authors

Konstantinos C. Tsolis, Mohamed Belal Hamed, Kenneth Simoens, Joachim Koepff, Tobias Busche, Christian Rückert, Marco Oldiges, Jörn Kalinowski, Jozef Anné, Jan Kormanec, Kristel Bernaerts, Spyridoula Karamanou, and Anastassios Economou

Correspondence

tassos.economou@kuleuven.be

Graphical Abstract

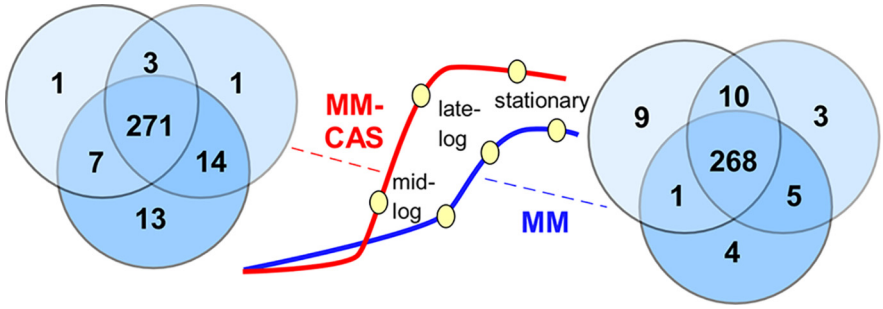

In Brief

Tsolis et al., reveal that the regulation of protein secretion in a Gram positive bacterial model is complex. Some of this regulation is transcriptional but a lot occurs post-transcriptionally and affects different exported proteins in different ways. Main Sec and chaperone machineries are not part of this regulation.

Highlights

- Stable and variable secretomes detected in a Gram$^+$ bacterial model.
- Quantitative and qualitative changes to a secretome subset.
- Transcriptional regulation but not export machinery levels account for secretome changes.
- Unknown post-transcriptional mechanisms link metabolism to secretion.

Tsolis et al., 2019, Molecular & Cellular Proteomics *18*, 423–436
March 2019
https://doi.org/10.1074/mcp.RA118.000899

Secretome Dynamics in a Gram-Positive Bacterial Model*[S]

Konstantinos C. Tsolis‡, Mohamed Belal Hamed‡‡, Kenneth Simoens§, Joachim Koepff¶, Tobias Busche‖, Christian Rückert‖, Marco Oldiges¶, Jörn Kalinowski‖, Jozef Anné‡, Jan Kormanec§§, Kristel Bernaerts§, Spyridoula Karamanou‡, and Anastassios Economou‡¶¶**

Protein secretion is a central biological process in all organisms. Most studies dissecting bacterial secretion mechanisms have focused on Gram-negative cell envelopes such as that of *Escherichia coli*. However, proteomics analyses in Gram negatives is hampered by their outer membrane. Here we studied protein secretion in the Gram-positive bacterium *Streptomyces lividans* TK24, in which most of the secretome is released in the growth medium. We monitored changes of the secretome as a function of growth phase and medium. We determined distinct protein classes of "house-keeping" secreted proteins that do not change their appearance or abundance in the various media and growth phases. These comprise mainly enzymes involved in cell wall maintenance and basic transport. In addition, we detected significant abundance and content changes to a sub-set of the proteome, as a function of growth in the different media. These did not depend on the media being minimal or rich. Transcriptional regulation but not changes in export machinery components can explain some of these changes. However, additional downstream mechanisms must be important for selective secretome funneling. These observations lay the foundations of using *S. lividans* as a model organism to study how metabolism is linked to optimal secretion and help develop rational optimization of heterologous protein production. ***Molecular & Cellular Proteomics 18: 423–436, 2019. DOI: 10.1074/mcp.RA118.000899.***

Bacterial protein secretion is a complex process that has been intensively dissected in the Gram-negative bacterial model cell *Escherichia coli* (1). All proteins that use the cell's export systems comprise the "exportome." These proteins can then either be inserted into the membrane (integral membrane proteins; "membranome") or can be completely translocated across it ("secretome"). This process is less well understood in Gram-positive bacteria in which secreted proteins are released to the culture medium after passing through one membrane and a thick peptidoglycan layer. The two major pathways for secretion of unfolded (Sec) or folded (Tat) proteins are highly conserved across Gram-positive and negative bacteria (2–4). However, several differences exist including *e.g.* the lack of SecB in the Gram positives, the presence of a second gene copy for YidC2, a fused SecDF protein, the use of sortases and multiple signal peptidases etc (5–7).

The Gram-positive *Streptomycetes* have sophisticated differentiation patterns (8, 9), very large proteomes of $>$ 7000 genes (10, 11), and complex metabolic networks, best known for their exploitation toward the production of chemicals of biomedical importance such as antibiotics (8, 12). *Streptomyces lividans* TK24 is a formidable platform for the heterologous secretion of several polypeptides of bacterial and eukaryotic origin using its Sec or Tat secretion systems (13–18). Its endogenous protein secretion mechanisms are poorly understood but, commonly, heterologous genes are fused to Sec signal peptide sequences from highly expressed/secreted endogenous *Streptomyces* proteins (2, 19, 20). The resulting proteins are thus targeted to the Sec pathway and, in many cases, efficiently secreted directly into the growth medium. The absence of lipopolysaccharides, the advanced genetic manipulation tools (18, 21), the established bioprocessing regimes (22–24), the low protease activity and the avoidance of inclusion body formation, render *S. lividans* secretion an attractive biotechnology platform. In many instances, it can provide alternative solutions replacing established workhorses, like *E. coli* (2).

Previously, it was demonstrated that *S. lividans* can efficiently secrete active trimeric murine tumor necrosis factor

From the ‡KU Leuven, Rega Institute, Dpt of Microbiology and Immunology, Herestraat 49, B-3000 Leuven, Belgium; §KU Leuven, Bio- & chemical systems Technology, Reactor Engineering and Safety Section, Department of Chemical Engineering, Celestijnenlaan 200F, 3001 Leuven, Belgium; ¶Forschungszentrum Jülich GmbH, Institute of Bio- and Geosciences, IBG-1: Biotechnology, Leo-Brandt-Straβe, 52428, Jülich, Germany; ‖Center for Biotechnology (CeBiTec), Bielefeld University, Bielefeld, Germany; **Institute for Biology-Microbiology, Freie Universität Berlin, Berlin, Germany; ‡‡Molecular Biology Dpt, National Research Centre, Dokki, Giza, Egypt; §§Institute of Molecular Biology, Slovak Academy of Sciences, Dubravska cesta 21, 84551 Bratislava, Slovakia

Received June 4, 2018, and in revised form, November 21, 2018
Published, MCP Papers in Press, November 29, 2018, DOI 10.1074/mcp.RA118.000899

alpha (mTNFα)[1] (16, 25), a *Jonesia* sp. xyloglucanase of 100 kDa (17), an extremely thermostable cellulase (26) and other polypeptides such as phospholipase D (15), transglutaminase, β-1,4-endoglucanase and β-glucosidase (27) into the growth medium. A successful approach we followed over the years has been the use of the transcription elements and the signal peptide of the *S. venezuelae* CBS762.70 subtilisin inhibitor gene (28). Despite their positive outcome, these efforts are, in essence, empirical. Secretion of several heterologous proteins is very poor suggesting that the elements that control what appears to be a complex pipeline, are not understood in depth. As an example of this, although signal peptides were traditionally considered as *passe-partout* elements, we have recently revealed that both the specific mature domain sequence to which they are attached and, more importantly, the conformational effects that this fusion has on the ensemble of the non-folded ensemble of the exported protein are crucial in deciding secretion (1, 29, 30).

One consistent observation in many of the studies of heterologous protein secretion as well as in the proteomics of the secretome (31), has been that protein secretion in *Streptomyces* appears to be remarkably dynamic and is obviously under complex regulation. Such complex regulation has not been observed in *E. coli* and may be characteristic for the class of Actinobacteria (32). Quantitative proteomics of *E. coli* grown in 22 different media/conditions revealed only marginal changes to the abundance of its Sec pathway genes (33) (data not shown). Monitoring the 505 proteins of the *E. coli* secretome revealed that 80% of them also do not undergo major abundance fluctuations. Moreover, protein secretion appears to be negatively-correlated with directing carbon flows to biomass production. In certain media that promote only poor cell growth, avid secretion of both endogenous and heterologous proteins is observed but the metabolic basis of this regulation is not clear (26).

To gain further insight in the molecular basis of how secretion can be regulated in such an apparently complex way and at which level, we characterized the dynamics of the *S. lividans* TK24 secretome across different experimental growth conditions using mass spectrometry and followed transcriptome changes by RNAseq. By combining the proteomics results with the latest annotation of the *S. lividans* TK24 proteome (34), we categorized the proteins based on their change in abundance either across the growth curve and/or across different media and chromosomal gene deletions and defined a "stable" and a "variable" proteome. Although significant differences are observed in "secretability," these do not correlate with changes in the production of export system genes and chaperones which seem to remain in rather stable amounts. Although for some secretome genes, transcriptional changes can directly account for secreted protein abundance changes, for many others they cannot. Rather, "secretability" appears to be regulated at downstream, currently unknown steps that allow specific funneling of some exported proteins for secretion but not of others. The current characterization of the dynamic behavior of the *S. lividans* secretome contributes to a first system's level understanding of its regulation. It is also an important first step for the use of *Streptomyces* as a cell factory for rationally designed heterologous protein production particularly combined with metabolomics data.

EXPERIMENTAL PROCEDURES

Bacterial Strains and Media Used—*Streptomyces lividans* TK24, a plasmid-free derivative of *S. lividans* 66 was used as a wild type (35).

Deletion of sigma factors and proteases genes listed in Table S8 described elsewhere (31). In addition, selected sigma factors genes or operons (Table S8, rows 9–13) in *S. lividans* TK24, were deleted using the pAMR12 deletion system described previously (36), based on the positive selection of double crossover events (37).

Media used in this study as described in (26) were: Phage medium (38) (per liter: 10 g Glucose, 5 g Tryptone, 5 g yeast extract, 5 g Lab Lemco powder, 0.74 g $CaCl_2.2H_2O$, 0.5 g $MgSO_4.7H_2O$, pH: 7.2), Minimal Medium (MM) (per liter: 10 g Glucose, 3 g $(NH_4)_2SO_4$, 2.6 g K_2HPO_4, 1.8 g NaH_2PO_4, 0.6 g $MgSO_4.7H_2O$, 25 ml minor elements solution (per liter: 40 mg $ZnSO_4.7H_2O$, 40 mg $FeSO_4.7H_2O$, 40 mg $CaCl_2$, 40 mg $MnCl_2.4H_2O$), Minimal medium with 5 g/L (MM_{C5}) and Nutrient Broth (NB) without NaCl [per liter: 8 g Nutrient Broth pH 6.9 (containing 5 g/L peptic digest of animal tissue, 3 g/L beef extract)].

Cell Growth in Micro- and Laboratory-scale Bioreactors—Strain cultivations were performed in a microbioreactor using 48 well FlowerPlates, covered by a gas-permeable sealing foil (Biolector system; m2p-labs GmbH, Baesweiler, Germany) (39). 1000 μl cultivation medium was inoculated to a final OD_{600} of 0.2. Temperature and humidity was controlled in the incubation chamber of the microbioreactor at 30 °C and 89% respectively. All signals (back-scattered light, DO, and pH), were measured with a cycle time of around 10 min.

The lab-scale bioreactor cultivations were carried out in an Eppendorf DASGIP Parallel Bioreactor System using 2,3 L vessels containing 1 L medium (at 30 °C; fixed stirring at 500 rpm; pH 6.8 maintained with 4 M KOH and 2 M H_2SO_4; air supply of 1 sL/min).

Dry Cell Weight Determination—Dry cell weight (DCW) for mircrotiter plate-based BioLector (BL) cultivations was determined using 800 μl of a well-mixed culture suspension, which was poured on pre-dried and pre-weighted spin down filter tubes (cellulose-acetate membrane; cut-off 0.2 μm; Corning). The supernatant was removed and harvested by filtration of the tubes on a TeVacs vacuum station (Tecan, Männedorf, Switzerland) with 700 mBar pressure difference. The biomass on the filters was additionally washed by adding 800 μl 0.9% w/v NaCl and a final wash step with water. Subsequently, the tubes were air-dried at 80 °C for 24 h and cooled down to room temperature before being weighted again on a precision scale (Type WZA215-LC, Sartorius Göttingen, Germany).

[1] The abbreviations used are: mTNFα, Murine tumor necrosis factor-alpha; ABS, Ammonium bicarbonate solution; CAN, Acetonitrile; BH, Benjamini and Hochberg; CBB, Coomassie brilliant blue; CID, Collisional induced dissociation; DTT, Dithiothreitol; DDA, Data-Dependent Acquisition; FA, Formic Acid; FDR, False discovery rate; FWHM, Full-width half maximum; iBAQ, Intensity based absolute quantification; LC-MS, Liquid chromatography–mass spectrometry; MM, Minimal medium; MM-CAS, Minimal medium supplemented with casamino acids; NB, Nutrient Broth Medium; NCE, Normalized collision energy; Ph, Phage medium; STAGE, Stop and go extraction; Tat, Twin-arginine translocation pathway; TCA, Trichloroacetic acid; TFA, Trifluoroacetic acid; TPM, Transcripts per kilobase million.

For lab-scale cultivations, DCW was measured as described (26). 10 ml of culture was centrifuged (falcon tubes; 3800 × *g*; 15 min; 3–16 K centrifuge Sigma). Pelleted cells were collected, resuspended in sterilized water and filtered under vacuum using a pre-dried and pre-weighted filter (0.2 μm pore size MN PORAFIL® MV; MACHEREY-NAGEL GmbH & Co. KG). The filter was once more dried (overnight 12–24 h in an oven at 60 °C) and weighted for DCW determination.

SDS-PAGE Analysis—Extracellular protein fractions of cultures of *S. lividans* and its derivatives were obtained after centrifugal removal of cells (10 min, 4200 *x g*, 4 °C). Precipitation of the proteins in the supernatant was, where applicable, carried out with TCA (final concentration of 20% w/v; 4 °C) (40). Proteins were separated by SDS-PAGE and masses determined with the Precision Plus Protein™ Standard (All Blue; Bio-Rad, Berkeley, California). Proteins were visualized by Coomassie Brilliant Blue (CBB) or by silver staining (41).

Experimental Design and Statistical Rationale—For the proteomic characterization of the *S. lividans* secretome 6 to 8 biological repeats were prepared for each experimental condition (see supplemental Table S1 and supplemental Table S4 for the exact number of repeats). Each experimental condition is compared with the WT sample of the same dataset (for the mutant comparison) or with the WT sample in MM-CAS medium at late-log exponential phase (for the media comparison). For the comparison of the growth phases of the same medium, all possible pairwise comparisons were tested. Protein abundance values were log transformed to approximate normal distribution and pairwise comparisons were performed using Student's *t* test and comparing the mean fold change. Calculated *p* values were further adjusted for multiple hypothesis testing error (see Proteomics Data Analysis). Missing values were omitted and only proteins identified in at least 3 biological repeats were included in the subsequent analysis.

Sample Preparation for Proteomics Analysis—Volumes corresponding to the secreted material of an equal number of cells were used for comparisons. Secretome samples from cells grown in MM or MM-CAS media were digested in-solution. Protein samples were solubilized in 8 M Urea at 50 mM ABS in water. Samples were diluted with 50 mM ABS until 2 M final Urea concentration, reduced with 2 mM DTT (45 min; 56 °C), alkylated with 10 mM Iodoacetamide (45 min; 20 °C; in the dark) and digested overnight (14 h; 37 °C) with trypsin (Trypsin Gold, Promega, Fitchburg, Wisconsin) using 1/100 trypsin to enzyme ratio, assuming that every sample contains ~3 μg of total protein content. Samples from complex growth media (NB, Phage and the corresponding control MM-CAS) were separated by SDS-PAGE and in-gel digested. Volumes corresponding to an equal number of cells was resolved in 1D-SDS-PAGE (4% stacking gel, 12% separating gel; 29:1, w/w acrylamide/bisacrylamide), run for 1 cm, digested as previously described (42). Digested peptides were acidified in a solution containing 0.1% v/v trifluoroacetic acid (TFA), until pH <2, dried under vacuum during centrifugation (Speedvac Concentrator, SAVANT ISS441, Thermo Scientific, Waltham, Massachusetts) and desalted using STAGE tips (42, 43).

LC-MS/MS Analysis—Lyophilized peptide samples were first dissolved in an aqueous solution containing 0.1% v/v formic acid (FA) and 5% v/v ACN and were analyzed using nano-Reverse Phase LC coupled to a Q Exactive™ Hybrid Quadrupole - Orbitrap or Orbitrap Elite Hybrid Iontrap - Orbitrap mass spectrometer (Thermo Scientific, Bremen, Germany) through a nanoelectrospray ion source (Thermo Scientific, Bremen, Germany). Peptides were initially separated using a Dionex UltiMate 3000 UHPLC or an Thermo EASY-nLC™-1200 system on an EasySpray C18 column (Thermo Scientific, OD 360 μm, ID 50 μm, 15 cm length, C18 resin, 2 μm bead size) at a nanoLC flow rate of 300 nL/min. The LC mobile phase consisted of two different buffer solutions, an aqueous solution containing 0.1% v/v FA (Buffer A) and an aqueous solution containing 0.1% v/v FA and 80% v/v ACN (Buffer B). A 60-min gradient was used from Buffer A to Buffer B (percentages from each in parentheses below) as follows: 0–3 min constant (96:4), 3–35 min (65:35); 35–40 min (35:65); 40–41 min (5:95); 41–50 min (5:95); 50–51 min (95:5); 51–60 min (95:5). Peptides were analyzed in the Orbitrap QE or an Orbitrap Elite as separate complete experimental datasets. Orbitrap QE operated in positive ion mode (nanospray voltage 1.6 kV, source temperature 250 °C), in data-dependent acquisition (DDA) mode with a survey MS scan at a resolution of 70,000 FWHM for the mass range of 400–1600 *m/z* for precursor ions, followed by MS/MS scans of the top 10 most intense peaks with +2, +3, and +4 charged ions above a threshold ion count of 16,000 at a resolution of 35,000 FWHM. Orbitrap Elite was operated in positive ion mode (nanospray voltage 1.8 kV, source temperature 275 °C), in DDA mode with a survey scan at a resolution of 240,000 FWHM for a mass range of 375–1500 *m/z* for precursor ions, followed by MS/MS scans of the 20 most intense peaks with charge +2 or higher, above a threshold count of 500 at a resolution of 17,000 FWHM. MS/MS in Orbitrap QE was performed using normalized collision energy (NCE) of 25% with an isolation window of 3.0 *m/z*, an apex trigger 5–15 s and a dynamic exclusion of 10 s. In Orbitrap Elite, MS/MS collisional induced dissociation (CID) was performed using 35% NCE with an isolation window of 2.0 *m/z*, and a dynamic exclusion list of 30 s. Data were acquired with Xcalibur 2.2 software (Thermo Scientific).

Proteomics Data Analysis—Raw MS files from the mass spectrometer were analyzed by MaxQuant v1.5.3.30, a quantitative proteomics software package designed for analyzing large mass spectrometric data sets (44). MS/MS spectra were searched against the re-annotated *Streptomyces lividans TK24* proteome (10) (7505 proteins) and common contaminants, using the Andromeda search engine (45). Enzyme specificity was set to trypsin, allowing for a maximum of two missed cleavages. Dynamic (methionine oxidation and N-terminal acetylation) and fixed (S-Carbamidomethylation of cysteinyl residues) modifications were selected. Precursor ion mass tolerance was set to 20 ppm and fragment ion tolerance to 20 ppm for Orbitrap QE or 0.5 Da for Orbitrap Elite. Protein and peptide False Discovery Rate (FDR) were set to 1%. Peptide features were aligned between different runs and masses were matched ("match between runs" feature), with a match time window of 2 min and a mass alignment window of 20 min. Label-free, relative protein quantification was performed using the iBAQ algorithm through the MaxQuant software (44, 46).

Data analysis (filtering, transformation and statistical analysis) was performed using custom scripts in R language (47). Differentially abundant proteins across experimental conditions were selected after performing a Student's *t* test on $\log_2$ iBAQ values and comparing the mean fold change of protein abundance across the experimental conditions, for proteins that were detected in at least 3 biological repeats for each condition. *t* test *p* values were adjusted for multiple hypothesis testing error (48) using the Benjamini and Hochberg (BH) method (49), as described (42). Thresholds for the selection of differentially abundant proteins include an adjusted *p* value < 0.05 and fold difference > 2. Proteins detected in 3 or more biological repeats were tested for difference in abundance across experimental conditions. Missing values were omitted. Uniquely identified proteins, in a pairwise comparison, were considered the ones that were detected in 3 or more biological repeats of one condition and less than 3 in the other. Functional characterization of the detected proteins was performed based on the manually annotated proteome of *S. lividans* obtained from SToPSdb (http://www.stopsdb.eu) (34). Statistically significant functional terms were selected using a Fisher exact test using as a threshold a *p* value < 0.05. Hierarchical clustering was performed using "Manhattan" distance, on proteins that were identified across all the pairwise comparisons.

Transcriptomics Data Analysis—For the transcriptomics data analysis, bacterial culture samples were taken during the mid-log and late-log growth phase as well as after entry into the stationary phase. Harvesting and RNA isolation were performed as described previously (50). Samples from two different biological replicates, for each experimental condition tested, were isolated separately and pooled after quality control. The RNA quality was checked via an Agilent 2100 Bioanalyzer (Agilent Technologies, Böblingen, Germany) and a Trinean Xposesystem (Gent, Belgium) before and after rRNA depletion using the Ribo Zero rRNA Removal Kit for Bacteria (Epicenter, Madison, WI). The TruSeq Stranded mRNA Library Prep Kit from Illumina was used to prepare the cDNA libraries, which were then sequenced in paired-end mode on an Illumina HiSeq 1500 system with 28 respectively 70 bases read length.

Transcripts per kilobase million (TPM) (51) were calculated using ReadXplorer v.2.2 (52). For differential RNA-Seq analyses the signal intensity value (A-value) was calculated by average $\log_2$ (TPM) of each gene and the signal intensity ratio (M-value) by the difference of $\log_2$ (TPM). In cases where the TPM for a gene was 0, a TPM of 0.1 was used instead, to avoid $\log_2$ (0). To identify genes that were strongly transcribed and differentially expressed under at least one condition, the RNA-Seq data were filtered using a TPM cut-off of 100 and an M-value cut-off of $>$1.0 under at least one condition.

Miscellaneous—Chemicals were from Sigma. Bacto Soytone from DIFCO Laboratories.

RESULTS

Proteomics of the Secretome in Streptomyces lividans TK24—More than a third of a cell's proteome (30% in *S. lividans* TK24 (55)), uses the cell's export systems in order to be inserted into the plasma membrane or to be translocated across it (34). To gain an understanding of how the secretome of TK24 is regulated, we developed a LC-MS/MS proteomics pipeline. Preliminary steps of such preparations (39), a detailed presentation of the main components of our LC-MS/MS pipeline and the statistical analysis of the data have been presented (42). We first focused on TK24 cells growing in a minimal medium supplemented with glucose with or without additional casamino acids (26). To secure statistical robustness, 6–8 biological repeats were used for each determination, taken from 3 different time points of a typical growth curve (Fig. 1*A*; mid-log exponential, late-log exponential and stationary phases). SDS-PAGE analysis of the supernatants revealed that the secretome profiles contain significant amounts of exported proteins (Fig. 1*B*). Supernatants of growth media were analyzed using LC-MS/MS and proteome annotation from the SToPSdb (http://www.stopsdb.eu) (34) was used for the interpretation of the proteomics results.

Proteomics analysis allowed routine detection of ~1,000 proteins in each sample (Fig. 1*D* and 1*E*, supplemental Table S1). Of these, ~500 represented cytoplasmic and ~150 membrane "contaminants" that could have derived either from cell lysis, from incomplete removal of cells during harvesting of growth media supernatants or even represent non-classical secretion (55). Cytoplasmic protein contamination could be explained by possible electrostatic interaction of the cytoplasmic proteins with the positively charged cell wall (56). To accurately calculate cell lysis in our cultures we used a TK24 derivative expressing a non-secreted mRFP protein and determined it to be in the order of 2–4% of total mRFP synthesized (26). This cytoplasmic component is marginally increased in stationary phase cells to up to ~6%. Thus, after subtracting this minor population, our secretome samples reflect, mainly, truly secreted polypeptides. Hereafter, these cytoplasmic and membrane "contaminants" were removed from any subsequent analysis. We only focused on the ~350 proteins of the experimentally detected secretome that comprises 270 secreted and 80 lipoproteins (supplemental Table S1).

Secretome Analysis of TK24 Grown in Minimal Media—We next examined how secretome abundance changes over the cell's growth curve. We compared the secretome abundance of proteins detected in the three sampling points (mid-log exponential, late-log exponential and stationary phase), in the minimal medium (MM) (Fig. 2*A*–2*C*) and MM supplemented with casamino acids (MM-CAS) (Fig. 2*D*–2*F*, supplemental Table S1). A similar number of exported proteins, (298–310), were detected in at least 3 biological repeats of every time point for each growth medium (Fig. 2*A*/2*D*). From these proteins, $>$90% are commonly detected across all time-points and would represent a "stable" secretome.

To further understand the kinetics of secretome abundance across the growth curve, we performed a pairwise comparison of protein quantification across the growth phases of the same medium (see Experimental Procedures). We tested for proteins with statistically significant differences in abundance between the time-points, by loading a sample volume that corresponds to equal amount of dry cell weight and comparing the iBAQ quantification values (46) (supplemental Fig. S1). Secreted proteins can be grouped in three classes. Proteins that do not show any significant difference in levels across the time-points are considered "stable" across the growth phases (Fig. 2*B*/2*E* top). These correspond to ~70% (MM) and 17% (MM-CAS) of the total detected secretome. Proteins with higher or lower abundance in stationary phase over the mid-log exponential are labeled as "increasing" in stationary or "decreasing" in stationary, accordingly (Fig. 2*B*/2*E* middle/bottom, supplemental Table S2 and S3).

Functional analysis of these three protein classes revealed groups of proteins that show distinct abundance profiles depending on the growth phase. In MM, secretome proteins with increasing abundance in the stationary phase are enriched in proteins related to transport and contain fewer hydrolases compared with the other two classes (see Experimental Procedures"). In MM-CAS, we observed significant differences in the number of transport-related proteins between the stable secretome and the proteins that increase in abundance toward the stationary phase, presumably reflecting the change in available compounds from the rich casamino acids mixture.

Secretome Changes Across Different Growth Regimes and Genetic Backgrounds—An alternative approach to examining secretome stability is to grow the cells under different media

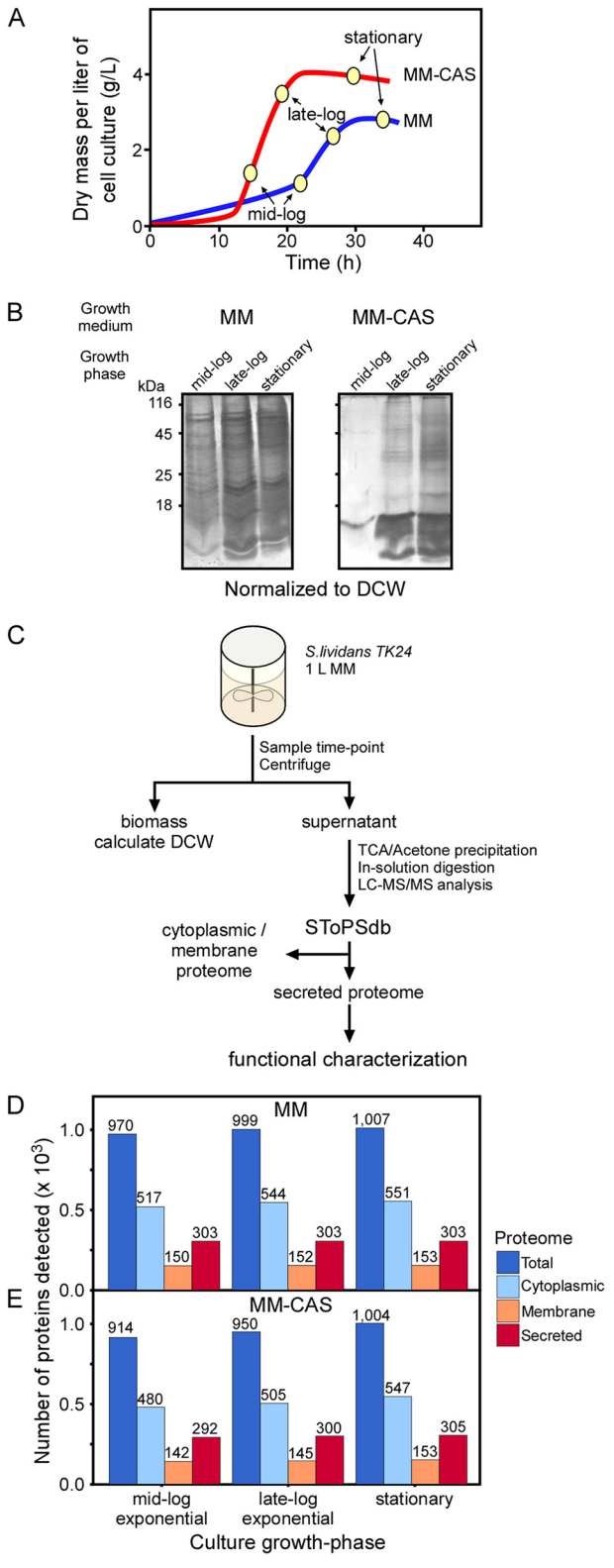

FIG. 1. **Experimental workflow for the proteomic characterization of the *S. lividans* secretome.** *A*, Representative growth curve of WT *S. lividans* TK24 growing in a 1 L bioreactor in MM or MM-CAS medium. Samples were taken at three time points during the growth (mid-log, late-log and stationary phases). *B*, Protein profile of the culture medium. Proteins present in the culture supernatant, for the corresponding sampling points were concentrated via TCA/acetone precipitation and were resolved in an SDS-PAGE gel. *C*, Experimental workflow used for the proteomic characterization of *S. lividans* TK24 secretome using mass spectrometry. $n = 8$ biological repeats for each time point for were used for all experimental conditions except MM-CAS mid-log phase where $n = 6$ (see supplemental Table S1 and supplemental Table S4 for absolute number per experimental condition). The sub-cellularly annotated proteome from SToPSdb was used to classify and functionally characterize the detected secreted proteins. Number of proteins detected at each time point as a total number, cytoplasmic, membrane or secreted for MM (*D*) or MM-CAS (*E*) growth media.

or to introduce genetic mutations that may influence their secretome profiles and compare the protein abundance across all these conditions. For this we focused on the late-log phase, growing cells in three media: a MM-CAS, that is considered our reference condition, phage medium (Ph), that is normally used for preparing bacterial inocula and shows poor secretion (26), and a nutrient broth medium (NB) shown to be the top performer in heterologous protein secretion/production (26) (Fig. 3*A*, supplemental Table S4/S5). Also, we compared the WT TK24 with derivatives that carry chromosomal gene deletion mutants of certain proteases or sigma factors. To facilitate direct comparison, all strains were grown in MM-CAS and we focused on the late-log phase only. Detailed discussion of the phenotype of the protease (31) or sigma factor deletion strains will be presented elsewhere.

For the purpose of this experiment, we minimized growth variability and non-uniform cell morphologies, a common problem in *Streptomyces* (57), by using a small-scale Bioelector system and examined 8 biological repeat samples from each medium. In this workflow cells can grow 48 parallel cultures that show a high degree of reproducibility (39). Following the same workflow as shown in Fig. 1*C*, pairwise comparison was performed for each experimental condition (medium/gene deletion) with the corresponding WT samples growing in MM-CAS. The number of exported proteins with differential abundance for each pairwise comparison, and the total number of exported proteins detected, is shown in Fig. 3*B*.

To evaluate the degree to which the different experimental conditions can affect the secretome protein levels, we first calculated the number of pairwise comparisons in which each protein shows similar abundance between the WT and the medium or gene deletion and summarized the frequencies in a histogram (Fig. 3*C*, supplemental Table S6). Based on the shape of the histogram (Fig. 3*C*) we split the proteins into two groups. Proteins that have similar abundance in >60% of the pairwise comparisons represent the "unaffected" or "stable" secretome. Proteins that are stable in <60% of the pairwise comparisons are considered as displaying abundances that are "affected" by the medium or the mutation. Almost 2/3 of these secreted proteins are unaffected across

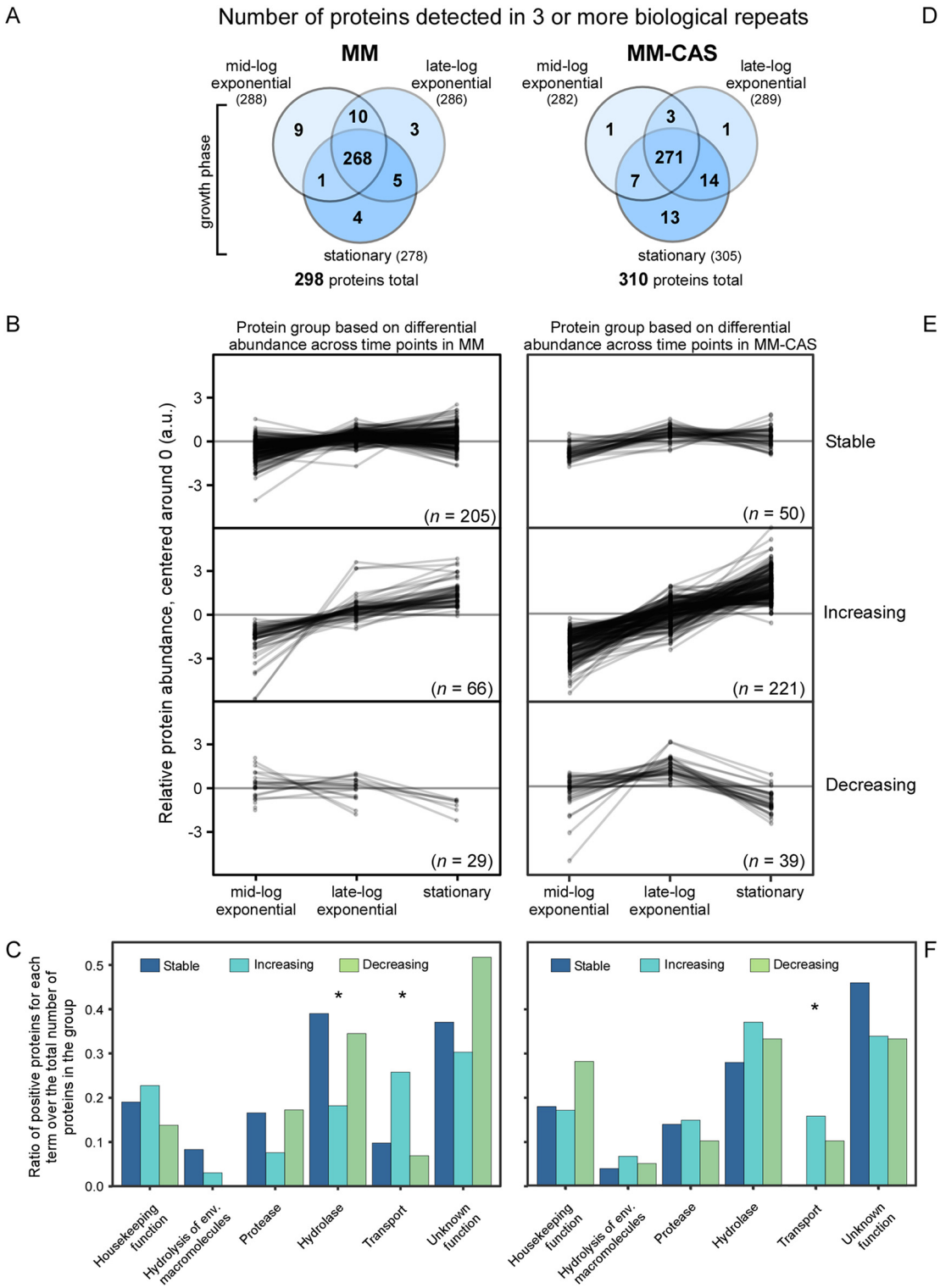

FIG. 2. **Stable and variable secretome of *S. lividans* over the growth curve.** Number of proteins detected at each time point in at least 3 biological repeats in MM (*A*) or in MM-CAS (*D*) growth media. Differential protein abundance for each time point of the same growth medium was tested after pairwise comparison between time points (see "Experimental procedures"). Identified proteins are classified into three categories based in their abundance (1. stable across the growth curve, 2. Increasing in abundance in stationary phase or 3. Decreasing in abundance in stationary phase). Each line represents the relative protein abundance over the growth for one protein, centered on 0, for MM (*B*) or MM-CAS (*E*). Functional characterization of the proteins of each category (see "Experimental procedures"), for MM (*C*) or MM-CAS (*F*). Statistically significant differences after a Fisher exact test are marked with an (*) (p value < 0.05).

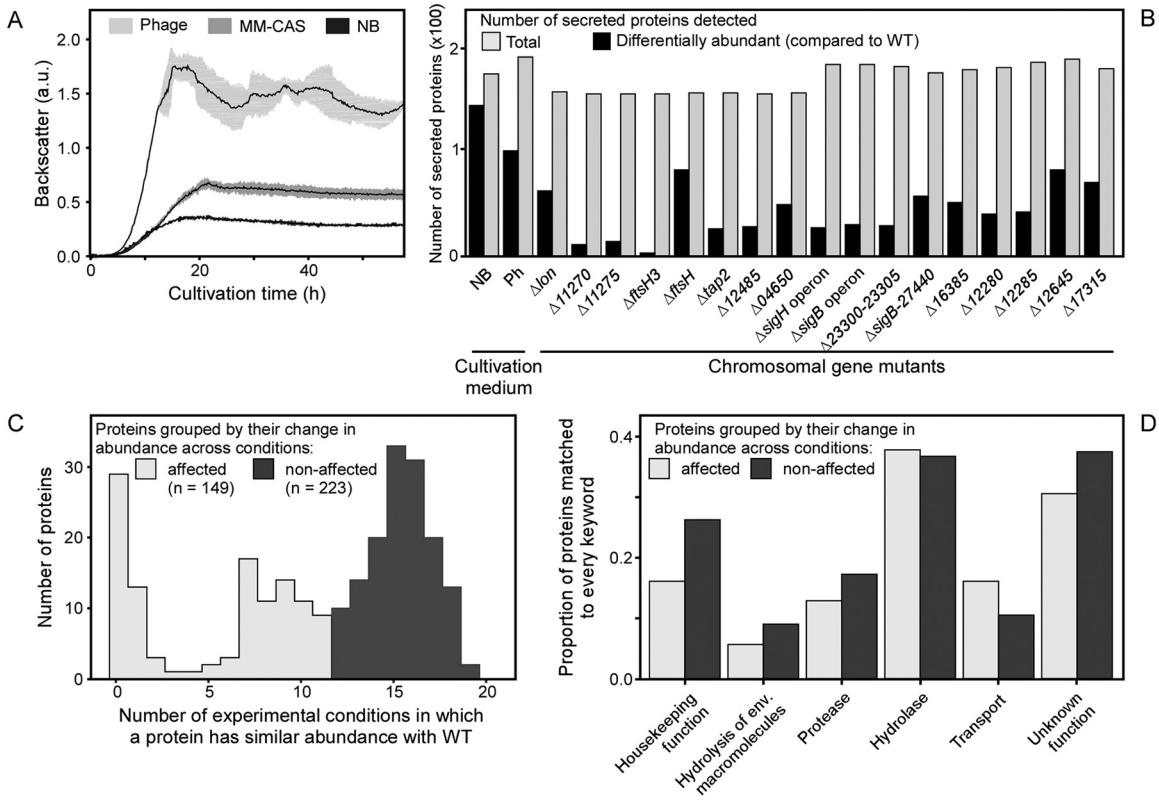

FIG. 3. **Secreted proteome changes across media and chromosomal gene deletions.** *A*, Representative growth curves of WT *S. lividans* TK24 growing in minimal medium complemented with casamino acids (MM-CAS), phage (Ph) or nutrient broth (NB) medium. *B*, Number of proteins with differential abundance compared with that of the WT condition (WT strain in MM-CAS), over the total number of secreted proteins, for each pairwise comparison. $n = 8$ biological repeats for each time point were used for all conditions except from NB and Ph media where $n = 7$. *C*, Frequency distribution of the number of pairwise comparisons each of the secreted proteins had similar abundance with the WT condition (WT strain in MM-CAS). Proteins with similar abundance with the WT in > 12 comparisons are considered as "non-affected" by the experimental conditions. *D*, Functional characterization of the secreted proteins that are "affected" or "non-affected" by the experimental condition. None of the comparisons shows statistically significant difference.

all our experimental conditions. Comparing the biological function of these two sub-proteomes we cannot conclude that there is a significant difference between these two groups for the functional terms that were examined (Fig. 3*D*, supplemental Table S6).

This analysis would suggest that specific proteins with a certain function rather than whole functional classes characterize the variable secretome. As an example of such specific changes in abundance, are the changes seen in one experimental condition, Δ*12285*, in which 116 proteins are synthesized in higher abundance presumably because the absence of this specific sigma factor gives rise to possible anti-sigma-factor effects (58).

Cell Mass and Protein Secretion Are Negatively Correlated—Over the course of several recent studies using TK24 (26, 31, 39) we observed that cells secreted more protein mass when they grew at slower growth rates. We extended this observation here by accumulating all available data from growth at different media, growth of mutants in protease genes (31), growth of mutants deleted in sigma factor genes and mutants of other regulatory elements (unpublished data) and built a composite graph in which dry cell weight of cell mass is plotted against total secreted protein corrected for cytoplasmic leakage as described previously (Fig. 4*A*). The data reveal a remarkable inverse-correlation of dry cell weight and total protein secretion measured. Apparently, excessive secretion is stimulated when carbon backbones cannot be metabolically funneled toward cell growth. Representative examples of secreted proteins from mutant derivatives/media that are negatively-correlated with the WT condition, can be identified by SDS-PAGE analysis (Fig. 4*B*). When the WT strain is grown in NB medium, the secretome profile shows significantly higher variation compared with the profile seen in MM-CAS medium. Most chromosomal gene deletions show a secretion profile that is more like that of the WT, however several protein bands seem to disappear or increase in intensity (Fig. 4*B*, asterisks).

The identified proteins show a characteristic pattern of increased or decreased abundance, across all the experimental conditions. We can cluster the secreted proteins using the output of each pairwise comparison with the WT and split them into three groups (Fig. 4*C*, supplemental Table S6). The

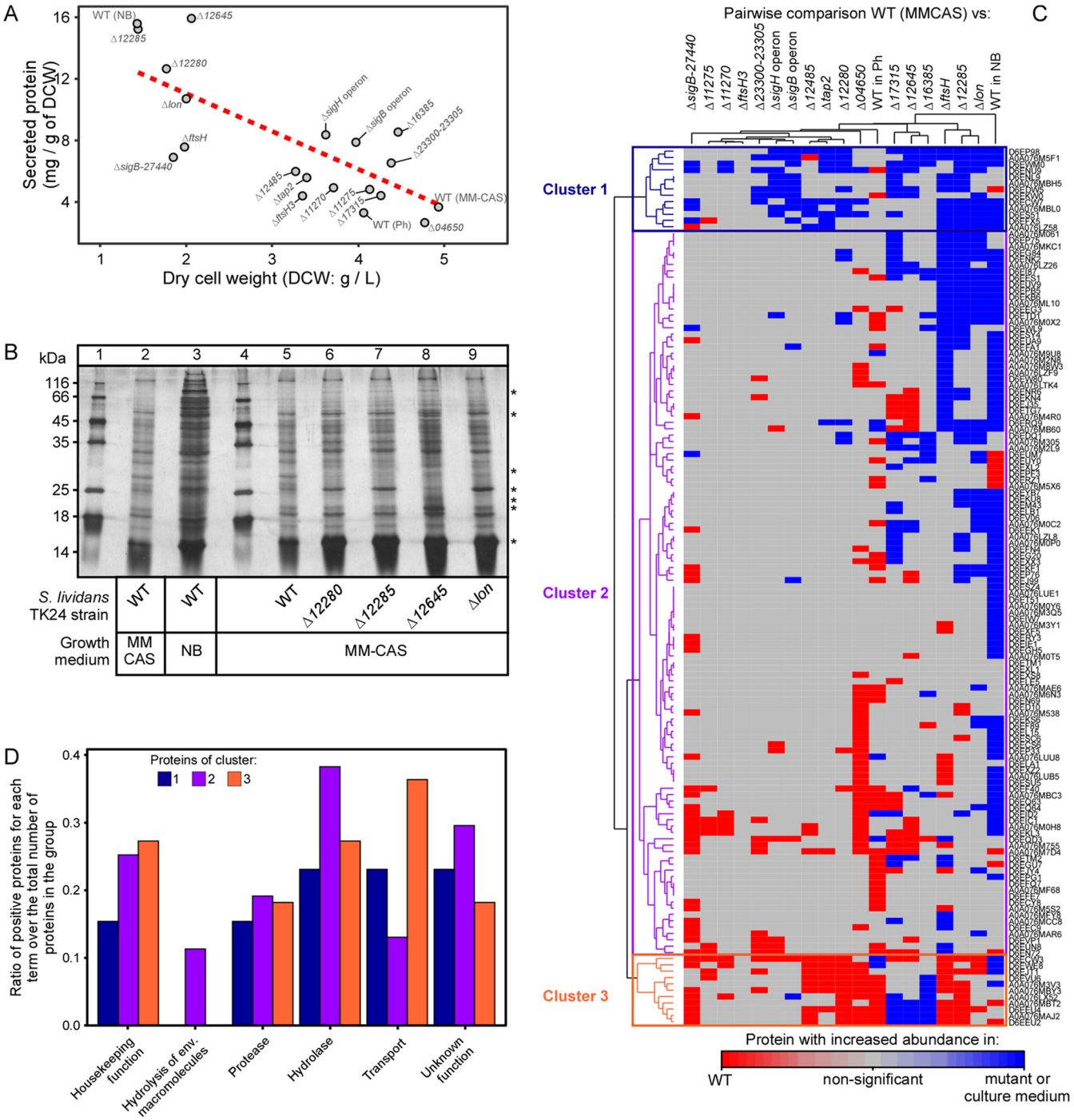

FIG. 4. **Global changes of the secreted proteins.** *A*, Correlation of dry cell weight and amount of secreted protein per dry cell weight for all the media or gene deletion strains described in this study. *B*, Supernatants from representative cultures with negatively-correlated ratios of secreted protein over dry cell weight compared with the WT conditions. SDS-PAGE gel stained with silver. *C*, Clustering of protein abundance across experimental conditions. Each column represents a pairwise comparison between the mutant/culture medium over the WT condition. Only secreted proteins identified across all samples are included in the heatmap. *D*, Functional characterization of the secreted protein clusters of panel (*C*). None of the comparisons shows statistically significant difference.

first cluster of proteins shows a more stable profile with protein levels like those of WT in most of the experimental conditions or with a balanced over-representation between WT and mutant/medium (cluster 1). The second cluster of proteins is primarily over-exported in the TK24 deletion mutants or the different culture media (cluster 2) and the third cluster exists in higher abundance in the WT condition (cluster 3). Even if none of the examined functional protein classes is considered sta-

tistically significant, when we compare these 3 clusters between them (Fig. 4*D*), this detailed labeling of the secreted proteome provides clues about the cell's response to different type of stimuli at the level of specific proteins. Detailed quantification for each protein across all the experimental conditions is provided in supplemental Table S2, S4 and (31).

Effect of Secretome Gene Transcription or Sec Machinery Expression On Export—The differences seen in protein abundance in the various conditions examined, result from unknown regulation. Two possible obvious mechanisms at play may be the change in transcription of certain secreted protein genes, *e.g.* expected in sigma factor gene deletions, in the change in levels of the secretion apparatus themselves or changes in chaperone abundance.

To examine this, we analyzed the transcriptomes of TK24 cells grown in two growth regimes, MM and MM-CAS media by RNASeq (Fig. 5, supplemental Fig. S2, supplemental Table S7). Transcript abundance of 746 secretome genes (98% of total) could be determined (supplemental Table S7). These include the transcripts of 464 of the secreted proteins unambiguously identified by MS (Fig. 5, supplemental Table S7). Among them, 257 and 174 transcripts (57 and 38%) follow trends like those seen for their secretome protein products in MM and MM-CAS respectively, *i.e.* they show elevated or reduced levels as their respective protein products (Fig. 5*C*). This good correlation suggests a simple mechanism by which transcription levels decide whether certain secreted proteins will be synthesized and made available for secretion. However, for a significant number of other secretome proteins (43% for MM and 62% for MMCAS) no such correlation is discernible. Secreted proteins can be exported at high levels in growth phase- or medium-dependent ways without their mRNAs showing any corresponding abundance changes (*e.g.* D6EP76 and D6EGL9; Fig. 5*B*). In such cases, simple transcriptional changes can no longer be invoked as the underlying regulatory mechanism and are suggesting of more complex downstream control.

One obvious target for post-transcriptional regulation of secretion is the protein export machineries of the cell. For this, we monitored transcript levels of the export machinery components of the two main export systems in TK24 (34): the Sec and the Tat systems, responsible for 93 and 7% of protein export respectively (34). Expression of most of these genes was found to be rather constant (Fig. 6*A*), with minor exceptions. The levels of *ftsY* expression, encoding a receptor for the Signal Recognition Particle, is more down-regulated in the MM-CAS media at later growth phases. *secE,* encoding a translocase channel component, is transcribed at lower levels in all phases of MM-CAS growth. *tig*, that encodes a general house-keeping chaperone that may play some role in secretion (59), shows reduced expression at later growth phases. Similar expression stability was seen for most Tat export components across growth phases and media (Fig 6*B*). Transcription of 37 genes encoding cell envelope potential chaperones and sortases (Fig 6*C*) also suggested minor changes in transcript levels. Similar results were seen with the minor Type VII export system (supplemental Fig. S2).

Finally, an additional level of secretion regulation may come via cytoplasmic chaperones. These could bind selectively to groups of secretory proteins and regulate their secretion, *e.g.* CspA (60). For this we examined the transcript levels of genes encoding 58 proteins of the cytoplasmic chaperonome (Fig. 6*C*, supplemental Table S7). These present a complex landscape that includes several stably and some variably expressed chaperone genes that might relate to regulating specific classes of exported proteins, but this cannot be discerned at this level of analysis.

We concluded that transcription-level changes may be a simple mechanism to explain protein abundance changes in the secretome. Nevertheless, the abundance changes in many more proteins are suggestive of more complex downstream mechanisms and remain unaccounted for against a background of rather stably expressed export pathway components and various potential chaperones. In addition, different turnover rates between proteins and transcripts because of their stability and accumulation kinetics can account for this variation (61, 62).

DISCUSSION

We present a systematic analysis of secretome dynamics by focusing on the Gram-positive bacterium *S. lividans* strain TK24, as a model system to analyze the regulation that underscores secretome biogenesis. Secretomes from a Gram-positive bacterium can be readily harvested from the growth medium and separated from other cellular contaminants.

Our approach has proven powerful in analyzing hundreds of secreted proteins simultaneously and determining which of these polypeptides can be considered as "house-keeping" proteins, constantly needed irrespective of growth conditions, in "stable" amounts and which others are needed on demand to degrade specific compounds in the medium or transport them inside the cell.

The secretome of TK24 changes in abundance over the cell's growth phases, in MM and MM-CAS media. In MM, the abundance of 70% of the secretome is stable over time, whereas in MM-CAS stable proteins represent only 16% of the total secretome. This variation could be explained by the composition of the culture media. MM only contains glucose as a carbon source and inorganic nitrogen sources. In contrast, MM-CAS has in addition several different carbon and nitrogen compounds present in the casamino acids hydrolysate. These become depleted in a differential manner over cellular growth (63) and may demand different enzymes and transport systems to be turned on during growth. This is also in agreement with the types of secretome proteins that are identified here, many of them including transporters and hydrolases (Fig. 2; supplemental Table S1).

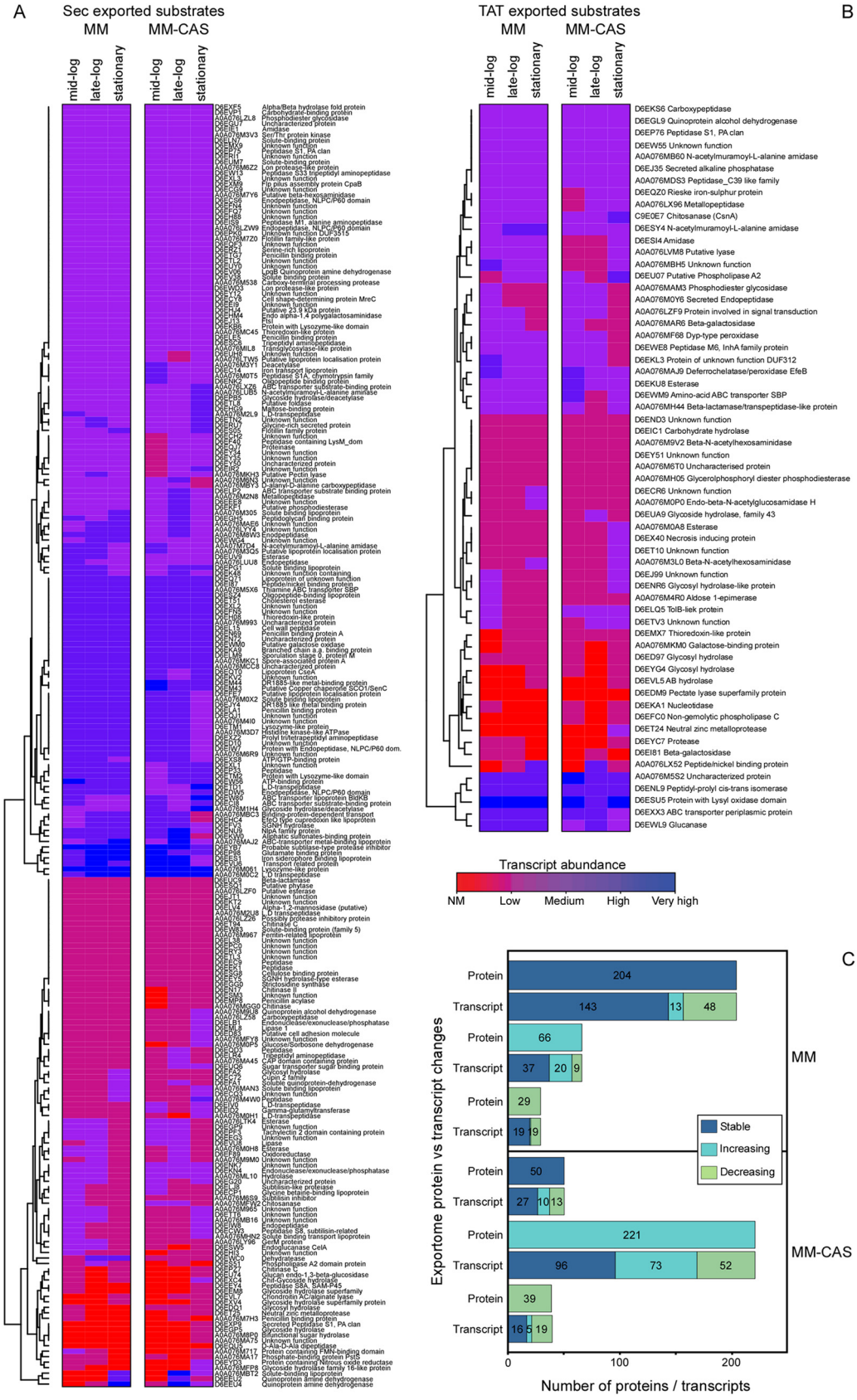

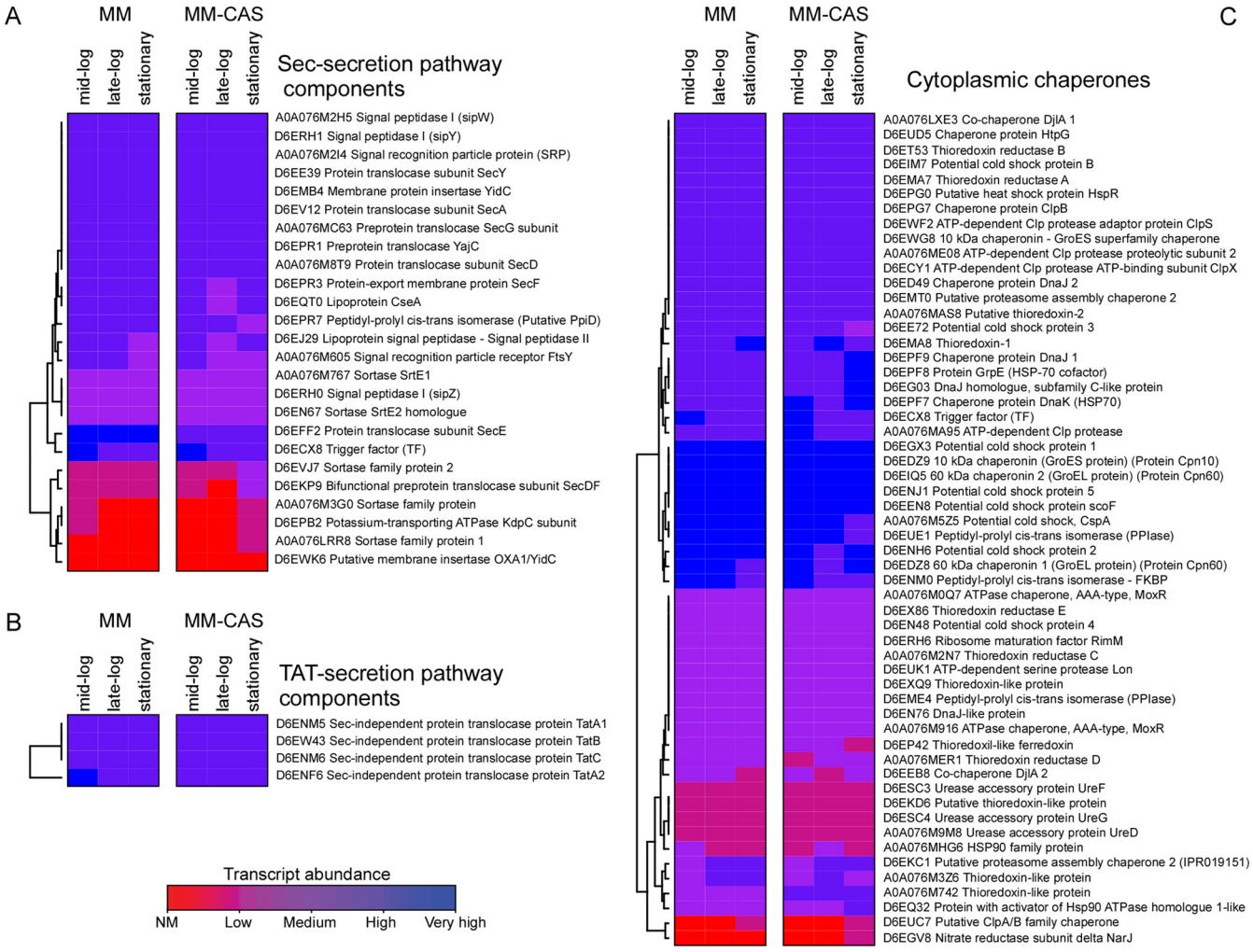

FIG. 6. **Transcriptome analysis of genes encoding protein export components.** Transcript abundance of the Sec export machinery components (*A*), the Tat export machinery components (*B*) and cytoplasmic chaperones (*C*) from cells grown in MM and MM-CAS media at the indicated growth phases determined as in Fig. 5.

Next, we studied the *S. lividans* secretome in three commonly used media and for multiple chromosomal gene deletions. Across these experimental conditions, we observe a consistently negative correlation between the total amount of secreted protein per unit cell-mass and the produced cell mass. Similar results have been reported in *Trichoderma reesei*, a filamentous fungus of industrial interest (64, 65). These observations are suggestive of selective funneling of carbon flows into secretome polypeptides that are then secreted. In our dataset, the two most extreme experimental conditions include TK24 growing in MM-CAS and NB medium. In MM-CAS we measured high cell mass and low amount of secreted protein per dry cell weight. In contrast, NB-grown cells produce high amount of secreted protein and low biomass. In various chromosomal gene deletions, the cells show intermediate phenotypes between those of the MM-CAS and NB media, suggesting that the absence of the deleted gene switched the cell's regulation, to a different extend, toward producing more secreted protein instead of cell mass. Moreover, cells with gene deletions showed a stable secretome that was comparable to that of TK24 (58% of total exported proteins identified by proteomics - Fig. 3*C*), suggesting that despite the obvious effects of gene deletions, the overall variable secretome is largely dictated by the growth medium. We hypothesize that a metabolome-secretome balance is a higher-level regulator of the system than the expression of

FIG. 5. **Transcriptome analysis of secretome genes.** Transcript abundance for the secretome proteins identified by proteomics (Fig. 1). $n = 6–8$ Two biological repeats for each condition and time point were used and merged into a single experimental data set and samples analyzed by RNAseq (31, 39). Transcripts are grouped based on the secretion system that their translated protein product uses for its export: *A*, Sec- and (*B*) Tat-secreted substrates. *C*, Comparison of transcript/protein abundance during the growth phase for MM and MM-CAS. Number of transcripts with stable increasing or decreasing abundance for each of the protein groups of Fig. 2 are calculated.

individual genes, but the molecular basis of these processes remains unknown.

A significant proportion of the secreted proteins seems to be unaffected by the experimental conditions applied. We refer to this as the "stable" secretome and is as important to determine as the "variable" one, as the former represents the secreted proteins that are part of the robustness of the cellular system. Approximately 2/3 of the identified proteins show similar abundance levels in the chromosomal gene deletion strains or in culture medium with the WT condition, pointing to a housekeeping secretome essential for cell proteostasis at all times. In addition, distinct protein clusters of the "variable" secretome increase or decrease in abundance when the experimental conditions are altered, providing evidence for possible pathways used by the cell in response to stationary phase adaptation and switching to secondary metabolite production as well as to adaptation to growth in different available carbon/nitrogen sources. Some of the secretome proteins show characteristic late stationary phase secretion (*e.g.* D6EI87: Peptide/nickel binding protein, MppA-type and D6EES1: Iron-siderophore binding lipoprotein). This raises the exciting hypothesis that secondary metabolite production networks may also be linked to specific needs in exported protein regulation. For the bacterial cell under study, this may involve secretome proteins involved in differentiation.

Although some of the changes seen in the "variable" proteome could be directly explained by transcriptional regulation (Fig. 5C), it is important to note that many others are suggestive of more complex, hitherto unknown, mechanisms that act post-transcriptionally. This could involve the use of specific chaperones forming transient sequestering pools, as trigger factor is seen to do in *E. coli* (59), or as the quasi "SecB chaperone analogue" CspA may do in Gram-positive bacteria that have no SecB (60). Another important aspect of the secretion potential of the cell involves the secretion pathway components. Despite the numerous secretome dynamics changes we have not come across conditions in which protein secretion ceases completely, even in the poorest media for secretion such as Phage medium (26). This would be expected given that secretion and the core Sec pathway genes are essential to maintain membrane and cell wall integrity, a proton gradient and peptidoglycan biosynthesis (66–68). Seeing that the variable proteome changes both in terms of abundance increase but also decrease, it would be intuitively expected that export translocases are always produced. This is also supported by the transcriptomics data that imply a rather constant production of most of these components. In summary, we expect that regulation of secretome dynamics is unusually complex and occurs only partly at transcription level and less likely at translocases level. A challenging and exciting future effort awaits the molecular understanding of these mechanisms and how selectivity for funneling specific groups of proteins to the export pathways can be achieved, whereas others are prevented from entering.

Our study provides a previously unavailable view of the complex regulation of protein secretion in bacteria, using a Gram-positive cell, with sophisticated differentiation and secondary metabolite programs, as a model. Combination of proteomics and transcriptomics efforts with metabolomics tools (63, 69) and location-biased protein targeting and secretion (70) are anticipated to allow mechanistic understanding of this fascinating process and reveal its regulatory elements.

Acknowledgments—We thank colleagues of the LMB and the StrepSynth consortium for useful discussions and the Sybioma facility (KU Leuven) for MS analysis.

DATA AVAILABILITY

The mass spectrometry proteomics data have been deposited to the ProteomeXchange Consortium via the PRIDE partner repository with the dataset identifiers PXD009675, PXD006819 and PXD006818 (53) and in the MS-Viewer repository with the dataset identifiers qo4plgjki0, oz5c3xvgfb, lhbdpbkug2, ptt8jkp6rn (54).

* This study was supported by the European Union project (grant E.U.-FP7 project 613877 "StrepSynth" to M.O., J.K., J.C., J.A., K.B. and A.E.), by the FWO (Fund for Scientific Research – Flanders; grant F.W.O. research project RiMembR to A.E.), the FWO/F.R.S.-FNRS "Excellence of Science-EOS" programme grant #30550343 (to A.E.), KU Leuven (#RUN/16/001; to A.E.) and by the VEGA grant 2/0002/16 from Slovak Academy of Sciences (to J.K.). H.M.B. is an Egyptian government doctoral fellow.

S This article contains supplemental Figures and Tables.

¶¶ To whom correspondence should be addressed: tassos.economou@kuleuven.be.

Author contributions: K.C.T. performed proteomics experiments, statistical analysis and analysis of transcriptomics data; H.M.B. performed cell growth and sample preparation for MS, SDS-PAGE analysis and cell mass determination; K.S., J.K., M.O., and K.B. provided secretome samples from large or small scale fermentation; J.K. generated knock-out strains; T.B., C.R., and J.K. provided transcriptomics data; S.K. and J.A. provided data analysis; K.C.T. and A.E. wrote the paper with contributions from H.M.B.; A.E. conceived, managed and supervised the project. All authors read and approved the MS.

REFERENCES

1. Sardis, M. F., Tsirigotaki, A., Chatzi, K. E., Portaliou, A. G., Gouridis, G., Karamanou, S., and Economou, A. (2017) Preprotein conformational dynamics drive bivalent translocase docking and secretion. *Structure* **25,** 1056–1067.e1056
2. Anné, J., Economou, A., and Bernaerts, K. (2017). "Protein secretion in gram-positive bacteria: from multiple pathways to biotechnology", in Protein and sugar export and assembly in gram-positive bacteria, eds. F. Bagnoli & R. Rappuoli. (Cham: Springer International Publishing), 267–308
3. Costa, T. R., Felisberto-Rodrigues, C., Meir, A., Prevost, M. S., Redzej, A., Trokter, M., and Waksman, G. (2015) Secretion systems in Gram-negative bacteria: structural and mechanistic insights. *Nat. Reviews. Microbiol.* **13,** 343–359
4. Green, E. R., and Mecsas, J. (2016) Bacterial Secretion Systems – An overview. *Microbiology spectrum* **4,** 10.1128/microbiolspec.VMBF-0012–2015
5. Schneewind, O., and Missiakas, D. M. (2012) Protein secretion and surface display in Gram-positive bacteria. *Philosophical Trans. Royal Soc. London. Series B, Biol. Sci,* **367,** 1123–1139

6. Zhou, Z., Sun, N., Wu, S., Li, Y. Q., and Wang, Y. (2016) Genomic data mining reveals a rich repertoire of transport proteins in *Streptomyces*. *BMC Genomics* **17,** 510
7. Goosens, V. J., Monteferrante, C. G., and van Dijl, J. M. (2014) The Tat system of Gram-positive bacteria. *Biochim. Biophys. Acta* **1843,** 1698–1706
8. van Wezel, G. P., and McDowall, K. J. (2011) The regulation of the secondary metabolism of *Streptomyces*: new links and experimental advances. *Natural Product Reports* **28,** 1311–1333
9. Chater, K. F., Biro, S., Lee, K. J., Palmer, T., and Schrempf, H. (2010) The complex extracellular biology of *Streptomyces*. *FEMS Microbiol. Rev.* **34,** 171–198
10. Ruckert, C., Albersmeier, A., Busche, T., Jaenicke, S., Winkler, A., Friethjonsson, O. H., Hreggviethsson, G. O., Lambert, C., Badcock, D., Bernaerts, K., Anné, J., Economou, A., and Kalinowski, J. (2015) Complete genome sequence of *Streptomyces lividans* TK24. *J. Biotechnol.* **199,** 21–22
11. Bentley, S. D., Chater, K. F., Cerdeno-Tarraga, A. M., Challis, G. L., Thomson, N. R., James, K. D., Harris, D. E., Quail, M. A., Kieser, H., Harper, D., Bateman, A., Brown, S., Chandra, G., Chen, C. W., Collins, M., Cronin, A., Fraser, A., Goble, A., Hidalgo, J., Hornsby, T., Howarth, S., Huang, C. H., Kieser, T., Larke, L., Murphy, L., Oliver, K., O'Neil, S., Rabbinowitsch, E., Rajandream, M. A., Rutherford, K., Rutter, S., Seeger, K., Saunders, D., Sharp, S., Squares, R., Squares, S., Taylor, K., Warren, T., Wietzorrek, A., Woodward, J., Barrell, B. G., Parkhill, J., and Hopwood, D. A. (2002) Complete genome sequence of the model actinomycete *Streptomyces coelicolor* A3(2). *Nature* **417,** 141–147
12. Liu, G., Chater, K. F., Chandra, G., Niu, G., and Tan, H. (2013) Molecular regulation of antibiotic biosynthesis in *streptomyces*. *Microbiol. Mol. Biol. Rev.* **77,** 112–143
13. Hong, B., Wu, B., and Li, Y. (2003) Production of C-terminal amidated recombinant salmon calcitonin in *Streptomyces lividans. Appl. Biochem. Biotechnol.* **110,** 113–123
14. Lara, M., Servin-Gonzalez, L., Singh, M., Moreno, C., Cohen, I., Nimtz, M., and Espitia, C. (2004) Expression, secretion, and glycosylation of the 45- and 47-kDa glycoprotein of *Mycobacterium tuberculosis* in *Streptomyces lividans. Appl. Environ. Microbiol.* **70,** 679–685
15. Ogino, C., Kanemasu, M., Hayashi, Y., Kondo, A., Shimizu, N., Tokuyama, S., Tahara, Y., Kuroda, S., Tanizawa, K., and Fukuda, H. (2004) Overexpression system for secretory phospholipase D by *Streptomyces lividans*. *Appl. Microbiol. Biotechnol.* **64,** 823–828
16. Pozidis, C., Lammertyn, E., Politou, A. S., Anné, J., Tsiftsoglou, A. S., Sianidis, G., and Economou, A. (2001) Protein secretion biotechnology using *Streptomyces lividans*: large-scale production of functional trimeric tumor necrosis factor alpha. *Biotechnol. Bioeng.* **72,** 611–619
17. Sianidis, G., Pozidis, C., Becker, F., Vrancken, K., Sjoeholm, C., Karamanou, S., Takamiya-Wik, M., van Mellaert, L., Schaefer, T., Anné, J., and Economou, A. (2006) Functional large-scale production of a novel Jonesia sp. xyloglucanase by heterologous secretion from *Streptomyces lividans*. *J. Biotechnol.* **121,** 498–507
18. Kashiwagi, N., Ogino, C., and Kondo, A. (2017) Production of chemicals and proteins using biomass-derived substrates from a Streptomyces host. *Bioresource Technol.* **245,** 1655–1663
19. Lammertyn, E., and Anné, J. (1998) Modifications of *Streptomyces* signal peptides and their effects on protein production and secretion. *FEMS Microbiol. Lett.* **160,** 1–10
20. Lammertyn, E., Desmyter, S., Schacht, S., Van Mellaert, L., and Anné, J. (1998) Influence of charge variation in the *Streptomyces venezuelae* alpha-amylase signal peptide on heterologous protein production by *Streptomyces lividans*. *Appl. Microbiol. Biotechnol.* **49,** 424–430
21. Kieser, T., Bibb, M. J., Buttner, M. J., Chater, K. F., and Hopwood, D. A. (2000) *Practical Streptomyces genetics.*, John Innes Foundation, Norwich, UK
22. Hwang, K. S., Kim, H. U., Charusanti, P., Palsson, B. O., and Lee, S. Y. (2014) Systems biology and biotechnology of *Streptomyces* species for the production of secondary metabolites. *Biotechnol. Adv.* **32,** 255–268
23. Chaudhary, A. K., Dhakal, D., and Sohng, J. K. (2013) An insight into the "-omics" based engineering of streptomycetes for secondary metabolite overproduction. *BioMed Res. Int.* **2013,** 968518
24. Hiltner, J. K., Hunter, I. S., and Hoskisson, P. A. (2015) Tailoring specialized metabolite production in *streptomyces*. *Adv. Appl. Microbiol.* **91,** 237–255
25. Lammertyn, E., Van Mellaert, L., Schacht, S., Dillen, C., Sablon, E., Van Broekhoven, A., and Anné, J. (1997) Evaluation of a novel subtilisin inhibitor gene and mutant derivatives for the expression and secretion of mouse tumor necrosis factor alpha by *Streptomyces lividans*. *Appl. Environ. Microbiol.* **63,** 1808–1813
26. Hamed, M. B., Karamanou, S., Olafsdottir, S., Basilio, J. S. M., Simoens, K., Tsolis, K. C., Van Mellaert, L., Guethmundsdottir, E. E., Hreggvidsson, G. O., Anné, J., Bernaerts, K., Fridjonsson, O. H., and Economou, A. (2017) Large-scale production of a thermostable *Rhodothermus marinus* cellulase by heterologous secretion from *Streptomyces lividans*. *Microbial. Cell Factories* **16,** 232
27. Noda, S., Ito, Y., Shimizu, N., Tanaka, T., Ogino, C., and Kondo, A. (2010) Over-production of various secretory-form proteins in *Streptomyces lividans*. *Protein Expression Purification* **73,** 198–202
28. Van Mellaert, L., Lammertyn, E., Schacht, S., Proost, P., Van Damme, J., Wroblowski, B., Anné, J., Scarcez, T., Sablon, E., Raeymaeckers, J., and Van Broekhoven, A. (1998) Molecular characterization of a novel subtilisin inhibitor protein produced by *Streptomyces venezuelae* CBS762.70. *DNA Seq* **9,** 19–30
29. Chatzi, K. E., Sardis, M. F., Tsirigotaki, A., Koukaki, M., Šoštarić, Konijnenberg, N. A., Sobott, F., Kalodimos, C. G., Karamanou, S., and Economou, A. (2017) Preprotein mature domains contain translocase targeting signals that are essential for secretion. *J. Cell Biol.* **216,** 1357–1369
30. Tsirigotaki, A., Chatzi, K. E., Koukaki, M., De Geyter, J., Portaliou, A. G., Orfanoudaki, G., Sardis, M. F., Trelle, M. B., Jorgensen, T. J. D., Karamanou, S., and Economou, A. (2018) Long-Lived Folding Intermediates Predominate the Targeting-Competent Secretome. *Structure* **26,** 695–707.e695
31. Busche, T., K. T. C., Koepff, J., Rebets, Y., Ruckert, C., Hamed, B. M., Bleidt, A., Wiechert, W., Lopatniuk, M., A., Anné Y. J., S. K, Oldiges, M., Luzhetskyy, J. K. A., and Economou, A. (2018) Multi-Omics and Targeted Approaches to Determine the Role of Cellular Proteases in *Streptomyces* Protein Secretion. *Frontiers Microbiol. (In press)*
32. Doroghazi, J. R., and Metcalf, W. W. (2013) Comparative genomics of actinomycetes with a focus on natural product biosynthetic genes. *BMC Genomics* **14,** 611
33. Schmidt, A., Kochanowski, K., Vedelaar, S., Ahrne, E., Volkmer, B., Callipo, L., Knoops, K., Bauer, M., Aebersold, R., and Heinemann, M. (2016) The Quantitative and Condition-Dependent *Escherichia coli* Proteome. *Nat. Biotechnol.* **34,** 104–110
34. Tsolis, K. C., Tsare, E. P., Orfanoudaki, G., Busche, T., Kanaki, K., Ramakrishnan, R., Rousseau, F., Schymkowitz, J., Ruckert, C., Kalinowski, J., Anne, J., Karamanou, S., Klapa, M. I., and Economou, A. (2018) Comprehensive subcellular topologies of polypeptides in *Streptomyces*. *Microbial Cell Factories* **17,** 43
35. Cruz-Morales, P., Vijgenboom, E., Iruegas-Bocardo, F., Girard, G., Yanez-Guerra, L. A., Ramos-Aboites, H. E., Pernodet, J. L., Anné, J., van Wezel, G. P., and Barona-Gomez, F. (2013) The genome sequence of *Streptomyces lividans* 66 reveals a novel tRNA-dependent peptide biosynthetic system within a metal-related genomic island. *Genome Biol. Evolution* **5,** 1165–1175
36. Novakova, R., Nunez, L. E., Homerova, D., Knirschova, R., Feckova, L., Rezuchova, B., Sevcikova, B., Menendez, N., Moris, F., and Cortes, J. (2018) Increased heterologous production of the antitumoral polyketide mithramycin A by engineered *Streptomyces lividans* TK24 strains. *Appl. Microbiol. Biotechnol.* **102,** 857–869
37. Knirschova, R., Novakova, R., Mingyar, E., Bekeova, C., Homerova, D., and Kormanec, J. (2015) Utilization of a reporter system based on the blue pigment indigoidine biosynthetic gene bpsA for detection of promoter activity and deletion of genes in *Streptomyces*. *J. Microbiol. Methods* **113,** 1–3
38. Korn, F., Weingärtner, B., and Kutzner, H. J. (1978) A study of twenty actinophages: morphology, serological relationship and host range. *E. Freerksen, I. Tarnok, J.H. Thumin (Eds.), Genetics of the Actinomycetales, Fisher G, Stuttgart*, pp. 251–270
39. Koepff, J., Keller, M., Tsolis, K. C., Busche, T., Ruckert, C., Hamed, M. B., Anné, J., Kalinowski, J., Wiechert, W., Economou, A., and Oldiges, M. (2017) Fast and reliable strain characterization of *Streptomyces lividans* through micro-scale cultivation. *Biotechnol. Bioeng.* In press

40. Mechin, V., Damerval, C., and Zivy, M. (2007) Total protein extraction with TCA-acetone. *Methods Mol. Biol.* **355,** 1–8
41. Shevchenko, A., Wilm, M., Vorm, O., and Mann, M. (1996) Mass spectrometric sequencing of proteins silver-stained polyacrylamide gels. *Anal. Chem.* **68,** 850–858
42. Tsolis, K. C., and Economou, A. (2017) Quantitative proteomics of the *E. coli* membranome. *Methods Enzymol.* **586,** 15–36
43. Rappsilber, J., Ishihama, Y., and Mann, M. (2003) Stop and go extraction tips for matrix-assisted laser desorption/ionization, nanoelectrospray, and LC/MS sample pretreatment in proteomics. *Anal. Chem.* **75,** 663–670
44. Cox, J., and Mann, M. (2008) MaxQuant enables high peptide identification rates, individualized p.p.b.-range mass accuracies and proteome-wide protein quantification. *Nature Biotechnol.* **26,** 1367–1372
45. Cox, J., Neuhauser, N., Michalski, A., Scheltema, R. A., Olsen, J. V., and Mann, M. (2011) Andromeda: a peptide search engine integrated into the MaxQuant environment. *J. Proteome Res.* **10,** 1794–1805
46. Schwanhausser, B., Busse, D., Li, N., Dittmar, G., Schuchhardt, J., Wolf, J., Chen, W., and Selbach, M. (2011) Global quantification of mammalian gene expression control. *Nature* **473,** 337–342
47. Core Team, R., and Computing, R. F. f. S (2017). R: A language and environment for statistical computing.
48. Diz, A. P., Carvajal-Rodriguez, A., and Skibinski, D. O. (2011) Multiple hypothesis testing in proteomics: a strategy for experimental work. *Mol. Cell. Proteomics* **10,** M110.004374
49. Benjamini, Y., and Hochberg, Y. (1995) Controlling the false discovery rate: a practical and powerful approach to multiple testing. *J. Royal Statistical Society.* **57,** 289–300
50. Busche, T., Silar, R., Picmanova, M., Patek, M., and Kalinowski, J. (2012) Transcriptional regulation of the operon encoding stress-responsive ECF sigma factor SigH and its anti-sigma factor RshA, and control of its regulatory network in *Corynebacterium glutamicum*. *BMC Genomics* **13,** 445
51. Wagner, G. P., Kin, K., and Lynch, V. J. (2012) Measurement of mRNA abundance using RNA-seq data: RPKM measure is inconsistent among samples. *Theory in biosciences = Theorie in den Biowissenschaften* **131,** 281–285
52. Hilker, R., Stadermann, K. B., Schwengers, O., Anisiforov, E., Jaenicke, S., Weisshaar, B., Zimmermann, T., and Goesmann, A. (2016) ReadXplorer 2-detailed read mapping analysis and visualization from one single source. *Bioinformatics* **32,** 3702–3708
53. Vizcaino, J. A., Csordas, A., Del-Toro, N., Dianes, J. A., Griss, J., Lavidas, I., Mayer, G., Perez-Riverol, Y., Reisinger, F., Ternent, T., Xu, Q. W., Wang, R., and Hermjakob, H. (2016) 2016 update of the PRIDE database and its related tools. *Nucleic acids Res.* **44,** 11033
54. Baker, P. R., and Chalkley, R. J. (2014) MS-Viewer: a web-based spectral viewer for proteomics results. *Mol. Cell. Proteomics* **13,** 1392–1396
55. Tsolis, K. C., Tsare, E.-P., Orfanoudaki, G., Busche, T., Kanaki, K., Ramakrishnan, R., Rousseau, F., Schymkowitz, J., Rueckert, C., Kalinowski, J., Anné, J., Karamanou, S., Klapa, I. M., and Economou, A. (2018) Sub-cellular topologies of polypeptides in *Streptomyces* (SToPSdb). *Microbial Cell Factory (In Press)*
56. Tiong, H. K., Hartson, S., and Muriana, P. M. (2015) Comparison of five methods for direct extraction of surface proteins from *Listeria monocytogenes* for proteomic analysis by orbitrap mass spectrometry. *J. Microbiol. Methods* **110,** 54–60
57. Jyothikumar, V., Tilley, E. J., Wali, R., and Herron, P. R. (2008) Time-lapse microscopy of *Streptomyces coelicolor* growth and sporulation. *Appl. Environ. Microbiol.* **74,** 6774–6781
58. Gehring, A. M., Yoo, N. J., and Losick, R. (2001) RNA polymerase sigma factor that blocks morphological differentiation by *Streptomyces coelicolor*. *J. Bacteriol.* **183,** 5991–5996
59. Saio, T., Guan, X., Rossi, P., Economou, A., and Kalodimos, C. G. (2014) Structural basis for protein antiaggregation activity of the trigger factor chaperone. *Science* **344,** 1250494
60. Keto-Timonen, R., Hietala, N., Palonen, E., Hakakorpi, A., Lindstrom, M., and Korkeala, H. (2016) Cold Shock Proteins: A Minireview with Special Emphasis on Csp-family of Enteropathogenic *Yersinia*. *Frontiers in Microbiol.* **7,** 1151
61. Swovick, K., Welle, K. A., Hryhorenko, J. R., Seluanov, A., Gorbunova, V., and Ghaemmaghami, S. (2018) Cross-species Comparison of Proteome Turnover Kinetics. *Mol. Cell. Proteomics* **17,** 580–591
62. Doherty, M. K., and Beynon, R. J. (2006) Protein turnover on the scale of the proteome. *Expert Rev. Proteomics* **3,** 97–110
63. Lule, I., D'Huys, P. J., Van Mellaert, L., Anné, J., Bernaerts, K., and Van Impe, J. (2013) Metabolic impact assessment for heterologous protein production in *Streptomyces lividans* based on genome-scale metabolic network modeling. *Mathematical Biosci.* **246,** 113–121
64. Pakula, T. M., Salonen, K., Uusitalo, J., and Penttila, M. (2005) The effect of specific growth rate on protein synthesis and secretion in the filamentous fungus *Trichoderma reesei*. *Microbiol.* **151,** 135–143
65. Arvas, M., Pakula, T., Smit, B., Rautio, J., Koivistoinen, H., Jouhten, P., Lindfors, E., Wiebe, M., Penttila, M., and Saloheimo, M. (2011) Correlation of gene expression and protein production rate - a system wide study. *BMC Genomics* **12,** 616
66. Alksne, L. E., Burgio, P., Hu, W., Feld, B., Singh, M. P., Tuckman, M., Petersen, P. J., Labthavikul, P., McGlynn, M., Barbieri, L., McDonald, L., Bradford, P., Dushin, R. G., Rothstein, D., and Projan, S. J. (2000) Identification and analysis of bacterial protein secretion inhibitors utilizing a SecA-LacZ reporter fusion system. *Antimicrobial Agents Chemotherapy* **44,** 1418–1427
67. Rajagopal, M., and Walker, S. (2017) Envelope Structures of Gram-Positive Bacteria. *Current Topics Microbiol. Immunol.* **404,** 1–44
68. Silhavy, T. J., Kahne, D., and Walker, S. (2010) The bacterial cell envelope. *Cold Spring Harbor Perspectives Biol.* **2,** a000414
69. Bouvin, J., Cajot, S., D'Huys, P. J., Ampofo-Asiama, J., Anné, J., Van Impe, J., Geeraerd, A., and Bernaerts, K. (2015) Multi-objective experimental design for (13)C-based metabolic flux analysis. *Mathematical Biosci.* **268,** 22–30
70. Yu, W., Missiakas, D., and Schneewind, O. (2018) Septal secretion of protein A in *Staphylococcus aureus* requires SecA and lipoteichoic acid synthesis. *eLife* **7,** e34092